EES Batteries

ROYAL SOCIETY OF CHEMISTRY

COMMUNICATION

View Article Online
View Journal

Cite this: DOI: 10.1039/d5eb00078e

Received 26th April 2025,
Accepted 9th May 2025

DOI: 10.1039/d5eb00078e

rsc.li/EESBatteries

Molecular dynamics of the coordination effect and ionic transport in TiO_2-filled poly(ethylene carbonate)-based electrolytes†

Wei Tan, [a] Kento Kimura [b] and Yoichi Tominaga *[a]

Solid composite electrolytes based on poly(ethylene carbonate) and rutile TiO_2 are investigated *via* molecular dynamics simulations. The incorporation of TiO_2 induces the formation of a space charge layer at the polymer–filler interface and facilitates low-resistance Li^+ hopping, significantly altering Li^+ coordination environments and leading to excellent local Li^+ mobility.

Broader context

This is the first report on the characterization of ionic mobility and solvation structure in Li salt-concentrated poly(ethylene carbonate) (PEC) electrolytes with TiO_2 using molecular modeling, calculations and simulations based on molecular dynamics, the radial distribution function and the free volume theory. Polymer electrolytes have attracted much attention as ion-conductive soft materials for novel battery systems because of their safety compared with liquid electrolytes, flexibility and light weight. We have already reported that highly salt-concentrated PEC electrolytes exhibit unique ion-conductive behavior (high conductivity, a high Li transference number t_+, excellent oxidation stability above 5 V, *etc.*) in the solid state. Moreover, we found that the composite electrolytes with inorganic fillers such as TiO_2 exhibit excellent properties such as increased Li^+ self-diffusion coefficients and t_+ values greater than 0.8. We believe that the presence of aggregated ions with moderately complex structures leads to favorable performance in such PEC-based electrolytes and that the interfacial ionic structure between the electrolyte phase and the TiO_2 surface may play an important role in enhancing ionic transport. We therefore focus on the computational characterization of PEC electrolyte models over a wide range of salt concentrations to understand the unusual solvation structure of ions.

Introduction

Since their commercial debut by Sony in the 1990s, lithium-ion batteries (LIBs) have become essential to modern society, serving as the primary power source for mobile phones, laptops, drones, and other portable electronic devices.[1–3] With continuous advancements in large-scale production and significant cost reductions, the energy density and specific energy of LIBs have surpassed 300 W h kg^{-1} and 750 W h L^{-1}, respectively, with further improvements driven by progress in materials science and manufacturing.[4,5] However, the growing electric vehicle (EV) market demands even higher energy densities, targeting over 500 W h kg^{-1}, to achieve driving ranges exceeding 1000 kilometres.[6]

Despite this increasing demand for high-capacity LIBs, several challenges remain, particularly concerning the lithium metal anode.[7,8] The weak bonding between lithium atoms not only facilitates the growth of lithium dendrites but also significantly increases the risks of internal short circuits and safety hazards.[9–11] Over the past decade, researchers have proposed various strategies to mitigate these issues, including advanced separators, electrolyte optimization, engineering of the interphase layer, and structural modifications of the anode.[12–15] Nevertheless, increasing the energy density inherently raises safety concerns. Therefore, replacing flammable liquid electrolytes with solid-state electrolytes has become a crucial focus for enhancing safety while meeting the demands for higher performance.

Solid electrolytes offer significant potential not only in mitigating dendrite formation but also in addressing critical instability in LIBs.[16,17] Among them, solid polymer electrolytes (SPEs), utilizing organic macromolecules such as poly(ethylene oxide) (PEO) or poly(ethylene carbonate) (PEC) as the polymer matrix, exhibit distinct advantages.[18,19] These include low density, excellent interfacial compatibility with electrodes, and favourable mechanical flexibility, making SPEs particularly

[a]*Graduate School of Bio-Applications and Systems Engineering (BASE), Tokyo University of Agriculture and Technology, 2-24-16 Nakacho, Koganei, Tokyo 184-8588, Japan. E-mail: ytominag@cc.tuat.ac.jp*
[b]*Department of Applied Chemistry, Graduate School of Engineering, Tokyo University of Agriculture and Technology, 2-24-16 Nakacho, Koganei, Tokyo 184-8588, Japan*

†Electronic supplementary information (ESI) available: Experimental details; Fig. S1; Tables S1–S3. See DOI: https://doi.org/10.1039/d5eb00078e

attractive for applications where weight reduction is essential, such as in EVs.

However, despite these advantages, a major challenge remains: the room-temperature ionic conductivity of SPEs typically falls within the range of 10^{-6} to 10^{-5} S cm^{-1}.[20,21] To overcome this limitation, extensive research has focused on developing solid composite electrolytes (SCEs) by introducing inorganic fillers into the polymer matrix. These fillers such as TiO_2 help lower the glass transition temperature of the polymer, disrupt its crystalline regions and promote the dissociation of lithium salts, thereby enhancing the segmental motion of polymer chains and increasing the concentration of free Li cations, significantly improving their mobility.[22–24] By synergistically combining the flexibility of polymers with the mechanical robustness of inorganic fillers, SCEs achieve better interfacial contact with electrodes while effectively suppressing lithium dendrite growth, paving the way for safer and more efficient high-energy-density batteries.

Nevertheless, a considerable gap still exists between the current performance of these materials and their theoretical potential, continuously driving researchers to seek breakthroughs through innovative technical strategies. One such approach is molecular dynamics (MD) simulations. MD simulations enable large-scale modelling that provides detailed and intuitive representations of lithium salt dissociation and ion transport dynamics.[25,26] This allows researchers to gain a clear understanding of how the introduction of fillers and their surface modifications affect Li^+ transport behaviour at the molecular level. Previous studies have demonstrated that incorporating TiO_2 into various polymer-based SCEs can significantly enhance metal ion conductivity and increase the Li^+ transport number.[27,28] Building on these findings, our study focuses on the role of TiO_2 in a system consisting of a PEC-based matrix and lithium bis(trifluoromethanesulfonyl)imide (LiTFSI). Composite models comprising PEC, LiTFSI and rutile TiO_2 were constructed through a multi-step process, as described in ESI.1,† with the separate models shown in Fig. 1. Moreover, MD simulations were employed to investigate the ionic behaviours in the SCE systems. This study systematically analysed the changes in the Li^+ coordination environment and ionic conductivity resulting from TiO_2 incorporation, providing an in-depth evaluation of how space charge layer (SCL) formation influences ion transport within the PEC-based composite electrolyte.

All simulations conducted in this work, including model construction and structure optimization, were performed using the Materials Studio[29] (MS) software package and its associated modules. MD simulations were executed using the Forcite module. Utilizing the COMPASS (Condensed-phase Optimized Molecular Potentials for Atomistic Simulation Studies) II force field, the Forcite module functions as a powerful molecular mechanics engine, enabling efficient energy calculations, structure optimization, and MD simulations, making it well suited for large-scale polymeric systems. COMPASS II is known for its extensive parameterization, combining empirical data with results from *ab initio* HF/6-31G* calculations to achieve high accuracy in simulating condensed-phase materials.[30,31] Numerous studies have demonstrated the applicability of COMPASS and Forcite in polymer and electrolyte research. For example, Amrhar *et al.* investigated the adsorption mechanisms of anionic dyes on the TiO_2 (110) surface,[32] and Ibrahim *et al.* simulated a graphene membrane/TiO_2 bilayer nanocomposite to enhance the electronic and mechanical properties of the graphene membrane.[33] These examples underscore the reliability and versatility of COMPASS II and support its use in this study for accurately capturing the structural and dynamic properties of the PEC-based electrolyte.

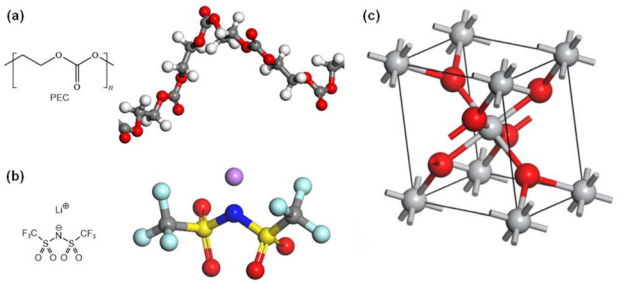

Fig. 1 Chemical structures and molecular models of (a) a PEC chain, (b) LiTFSI and (c) a unit cell of rutile TiO_2.

To balance accuracy and computational efficiency, appropriate functionals and methods were meticulously chosen for each calculation step, as detailed in ESI.2.† In addition, coordination structures and ionic mobility within the system were systematically analysed based on radial distribution function (RDF) and mean-square displacement (MSD) results (theoretical basis provided in ESI.3†). These data were extracted from MD simulations conducted under the NVT ensemble (where the number of atoms, volume, and temperature are conserved) and the NVE ensemble (where the number of atoms, volume, and energy are conserved), ensuring reliable characterization of dynamic behaviours.

Results and discussion

Following MD simulations, significant changes in the spatial distribution of ions within the electrolyte model were observed, as illustrated in Fig. 2. The initial model, constructed using a Monte Carlo-based method, exhibited a homogeneous spatial arrangement of the PEC backbone and both ion species (Li^+ and $TFSI^-$). However, after extensive 2000 ps NVT MD simulations, a substantial fraction of TFSI anions migrated toward the TiO_2 surface, forming a distinct interfacial region. This behaviour indicates a strong adsorption affinity of the rutile TiO_2 (110) surface for TFSI anions. Concurrently, partial displacement of the PEC backbone toward the TiO_2 surface was observed, albeit to a lesser extent compared to the TFSI anions. The adsorbed TFSI anions and PEC segments collectively formed an interface, leaving a

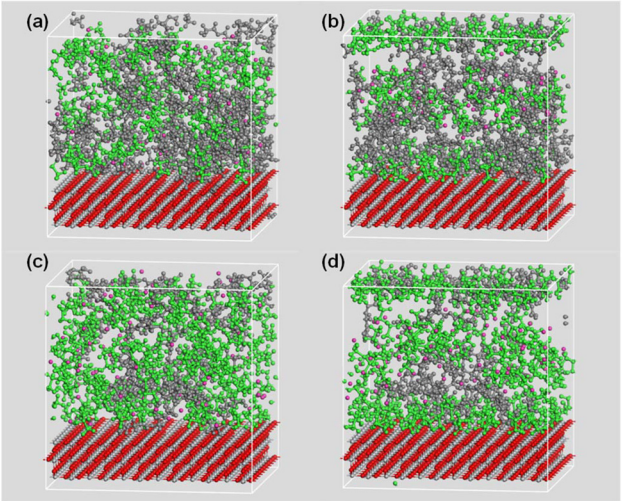

Fig. 2 TiO_2-filled PEC/LiTFSI SCE models under different conditions: (a) initial configuration of the 40 mol% model; (b) 40 mol% model after 2000 ps NVT MD simulation; (c) initial configuration of the 120 mol% model; and (d) 120 mol% model after 2000 ps NVT MD simulation. TFSI anions are shown in green, PEC chains in grey and Li cations in purple.

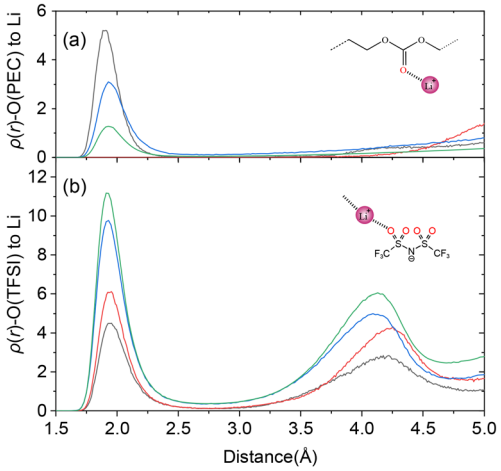

Fig. 3 RDFs simulated for PEC/LiTFSI SPE and TiO_2-filled SCE models between Li cations and oxygen atoms from (a) carbonyl groups in polymer chains and (b) TFSI anions. RDF curves are coloured based on salt concentration: 40 mol% SCE (black), 120 mol% SCE (red), 40 mol% SPE (blue) and 120 mol% SPE (green).

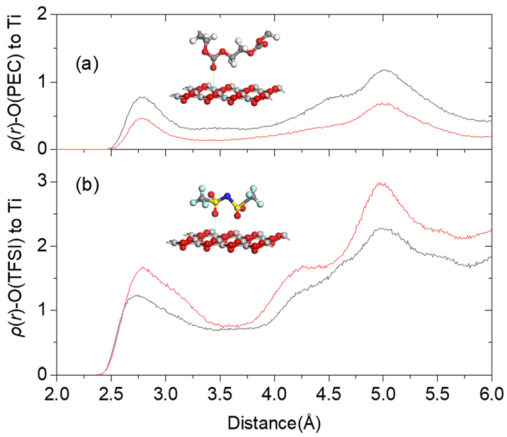

Fig. 4 RDFs simulated for TiO_2-filled PEC/LiTFSI SCE models between Ti atoms and oxygen atoms from (a) carbonyl groups in polymer chains and (b) TFSI anions. RDF curves are coloured based on salt concentration: 40 mol% (black) and 120 mol% (red).

narrow gap between this interface and the bulk region, corresponding to a SCL. In contrast, Li cations were predominantly localized within the bulk and SCL regions, avoiding proximity to the TiO_2 surface.

The RDFs of Li cations in PEC/LiTFSI electrolytes were calculated before and after TiO_2 addition, as shown in Fig. 3. Oxygen atoms from TFSI anions were denoted as O(TFSI), while carbonyl oxygen atoms from PEC were labelled as O(PEC). The results show a significant reduction in the coordination number (CN) between Li cations and O(TFSI) in both 40 mol% and 120 mol% salt concentration systems following TiO_2 incorporation. This reduction indicates that TiO_2 effectively suppresses Li–O(TFSI) coordination, thereby promoting Li^+ dissociation within the electrolyte. Additionally, a rightward shift of the second RDF peak is observed in TiO_2-containing systems, reflecting increased distances between TFSI anions, which is consistent with the formation of interfacial gaps in the model. For O(PEC), at a 40 mol% salt concentration, TiO_2 addition enhances Li–PEC interactions, evidenced by a leftward shift of the first RDF peak, suggesting stronger coordination. However, at 120 mol% salt concentration, the observation is counterintuitive and warrants further investigation: Li cations appear to completely lose interaction with PEC carbonyl oxygen atoms. This observation suggests that, within this interfacial system, the coordination environment of Li cations is dominated solely by O(TFSI).

In addition, we calculated the RDFs between Ti atoms on the TiO_2 (110) surface and the two types of oxygen atoms, O(TFSI) from TFSI anions and O(PEC) from the polymer, as shown in Fig. 4. The RDF profiles reveal that Ti exhibits adsorption interactions with both O(TFSI) and O(PEC), with a notably stronger affinity for O(TFSI). As the salt concentration increases from 40 mol% to 120 mol%, the adsorption of O(TFSI) is further enhanced, while the interaction with O(PEC) weakens. This trend is attributed to the increased relative abundance of TFSI anions at higher salt concentrations. Furthermore, the adsorption distances between Ti and both O(TFSI) and O(PEC) are approximately 2.7 Å, which is notably longer than the average Ti–O bond length within the rutile TiO_2 lattice (1.96 Å),[34] suggesting physisorption rather than chemisorption.

Based on the RDF data, we further calculated the CNs of Li cations corresponding to each RDF curve, as summarized in Table S1.† Following TiO_2 addition, the total CNs of Li cations decrease to 2.61 (40 mol%) and 1.79 (120 mol%), compared to 4.03 and 3.85 in the TiO_2-free systems. At a salt concentration

of 40 mol%, TiO_2 addition sharply reduces the Li–O(TFSI) CN from 2.97 to 1.39, while slightly increasing the Li–O(PEC) CN from 1.06 to 1.22. In contrast, at 120 mol% salt concentration, TiO_2 incorporation significantly decreases both Li–O(TFSI) and Li–O(PEC) CNs, with the latter dropping to 0. These reductions indicate weakened coordination interactions, which are expected to enhance Li^+ mobility. The formation of the SCL likely facilitates low-resistance hopping migration of Li cations, thereby improving ionic conductivity.[35,36] Notably, in the 120 mol% SCE system, Li^+ migration through the SCL occurs with minimal interaction with PEC, deviating from conventional hopping mechanisms. Additionally, the Ti–O(TFSI) CNs are 1.01 and 1.26 for the 40 mol% and 120 mol% systems, respectively, while the Ti–O(PEC) CNs decrease from 0.46 to 0.23. Notably, the total number of adsorbed oxygen atoms (from both TFSI anions and PEC) per surface Ti atom remains nearly constant at approximately 1.5 across both concentrations, suggesting that the overall adsorption capacity is robust and largely unaffected by salt concentration.

Due to Ti-induced adsorption interactions, the mobility of TFSI anions is inevitably impacted. To quantify this effect, TFSI anions were classified into two groups based on whether their oxygen atoms were adsorbed by Ti: TFSI(interface) and TFSI(bulk). The MSDs of Li^+ and both $TFSI^-$ groups in the TiO_2-containing PEC/LiTFSI system were subsequently calculated, as shown in Fig. 5. The results demonstrate that Li cations exhibit the highest MSD, followed by TFSI(bulk), while TFSI(interface) displays a significantly lower MSD than both, indicating restricted mobility due to surface adsorption.

Using the MSD data, we further calculated the ionic conductivity and transport numbers for each ion species. The logarithmic conductivity denoted as $\log \sigma$ and transport number results are summarized in Tables S2 and S3.† The results reveal that TiO_2 incorporation significantly enhances Li^+ conductivity. Notably, at a 40 mol% salt concentration, the Li^+ conductivity (2.12×10^{-4} S cm^{-1}) exceeds that of the TiO_2-free system at 120 mol%. Furthermore, the influence of salt concentration on Li^+ conductivity is markedly reduced in TiO_2-containing systems. Given the previously discussed stability of Ti adsorption interactions, the SCLs formed at 40 mol% and 120 mol% likely exhibit similar electrochemical properties, resulting in comparable resistance to Li^+ migration. In contrast, $TFSI^-$ conductivity decreases substantially upon TiO_2 addition. For TFSI(bulk), conductivity drops by approximately 20% at 40 mol% and 35% at 120 mol%, showing a clear declining trend. This decline may be attributed to the formation of the SCL, which compresses the free volume available for TFSI anions from the interface side. Reductions are even more pronounced for TFSI(interface), with conductivity decreasing by 53% at 40 mol% and 88% at 120 mol%, respectively. In TiO_2-free systems, the Li^+ transport numbers are 0.33 (40 mol%) and 0.55 (120 mol%). Upon TiO_2 addition, these values increase sharply to 0.79 (40 mol%) and 0.85 (120 mol%), indicating that TiO_2 suppresses anion migration, thereby altering the conduction mechanism and significantly enhancing the Li^+ transport number.

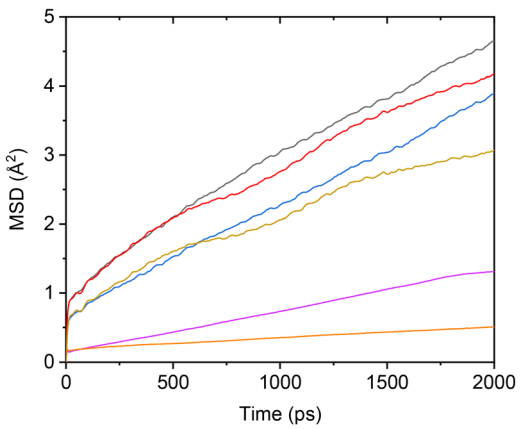

Fig. 5 MSDs simulated for TiO_2-filled PEC/LiTFSI SCE models under different conditions. Data are shown for Li^+ at salt concentrations of 40 mol% (black) and 120 mol% (red), TFSI(bulk) at salt concentrations of 40 mol% (blue) and 120 mol% (dark yellow), and TFSI(interface) at salt concentrations of 40 mol% (purple) and 120 mol% (orange).

Conclusions

In this study, MD simulations were employed to investigate the effects of rutile-TiO_2 incorporation on the interfacial structure and its subsequent influence on ionic coordination environments and mobility within PEC/LiTFSI electrolytes. Based on the simulation results, we propose that the addition of TiO_2 nanoparticles induces the formation of interfacial regions with reduced resistance and enhanced Li^+ transport properties within the PEC/LiTFSI SPE system. In the absence of TiO_2, Li cations migrate *via* hopping mechanisms governed by the dynamic formation and dissociation of coordination with the PEC backbone and TFSI anions. However, upon encountering TiO_2 nanoparticles, the presence of SCLs alters the ion transport pathway, leading Li cations to migrate preferentially *via* a modified hopping mechanism. In highly concentrated SCEs, Li^+ migration within the interfacial region involves only 1 or 2 TFSI anions in each dynamic process. It is important to note that, although the simulations yielded high ionic conductivity and a Li^+ transport number of up to 0.85, the constructed SCE models represent interfacial regions in close contact with TiO_2 nanoparticles. These models thus characterize the local environment rather than the entire TiO_2-filled composite electrolytes. The significantly improved ionic conductivity and elevated Li^+ transport number observed in the interfacial regions of SCEs are attributed to the optimized interfacial pathways, which facilitate more efficient Li^+ migration compared to the TiO_2-free systems. These effects highlight the potential of rutile TiO_2 nanoparticles in addressing critical challenges in solid-state batteries, including energy density limitations and safety concerns. The atomic-scale insights provided by this work underscore the importance of filler-engineered interfaces in optimizing polymer-based electrolytes.

Future studies should focus on extending MD simulations to investigate surface defects and long-term interfacial stability, which could further advance the design of high-performance, durable solid-state battery systems.

Author contributions

Conceptualization, W.T. and Y.T.; methodology, W.T.; software, W.T.; formal analysis, W.T.; writing – original draft, W.T.; writing – review and editing, K.K. and Y.T.; supervision, K.K. and Y.T.; and funding acquisition, Y.T. All authors have read and agreed to the published version of the manuscript.

Data availability

The data supporting this article have been included as part of the ESI.†

Conflicts of interest

There are no conflicts to declare.

Acknowledgements

This research was financially supported by a Grant-in-Aid for Scientific Research (B) (23K23057) of JSPS KAKENHI and the Data Creation and Utilization-Type Material Research and Development Project (JPMXP1122712807) of MEXT, Japan.

References

1 Y. Nishi, *J. Power Sources*, 2001, **100**, 101–106.
2 P. V. Kamat, *ACS Energy Lett.*, 2019, **4**, 2757–2759.
3 J.-M. Tarascon and M. Armand, *Nature*, 2001, **414**, 359–367.
4 H. Li, *Joule*, 2019, **3**, 911–914.
5 T. Waldmann, *et al.*, *J. Power Sources*, 2020, **472**, 228614.
6 J. Liu, *et al.*, *Nat. Energy*, 2019, **4**, 180–186.
7 D. Lin, Y. Liu and Y. Cui, *Nat. Nanotechnol.*, 2017, **12**, 194–206.
8 Y. Gao, *et al.*, *Nano-Micro Lett.*, 2022, **14**, 94.
9 I. Yoshimatsu, T. Hirai and J. Yamaki, *J. Electrochem. Soc.*, 1988, **135**, 2422.
10 C. Ling, D. Banerjee and M. Matsui, *Electrochim. Acta*, 2012, **76**, 270–274.
11 M. Rosso, *et al.*, *Electrochim. Acta*, 2006, **51**, 5334–5340.
12 D. Wang, *et al.*, *Adv. Sci.*, 2017, **4**, 1600168.
13 W. Xu, *et al.*, *Energy Environ. Sci.*, 2014, **7**, 513–537.
14 A. C. Kozen, *et al.*, *ACS Nano*, 2015, **9**, 5884–5892.
15 L. Fan, *et al.*, *Adv. Energy Mater.*, 2018, **8**, 1802350.
16 A. Manthiram, X. Yu and S. Wang, *Nat. Rev. Mater.*, 2017, **2**, 1–16.
17 P. Bonnick and J. Muldoon, *Energy Environ. Sci.*, 2022, **15**, 1840–1860.
18 J. Mindemark, *et al.*, *Prog. Polym. Sci.*, 2018, **81**, 114–143.
19 F. Wu, *et al.*, *Energy Storage Mater.*, 2020, **33**, 26–54.
20 D. Zhou, *et al.*, *Chem*, 2019, **5**, 2326–2352.
21 L. Yue, *et al.*, *Energy Storage Mater.*, 2016, **5**, 139–164.
22 S. Duan, *et al.*, *Adv. Mater.*, 2024, **36**, 2314120.
23 Y. Zheng, *et al.*, *Energy Storage Mater.*, 2023, **57**, 540–548.
24 H. Zhang, *et al.*, *Chem. Soc. Rev.*, 2017, **46**, 797–815.
25 M. Yao, *et al.*, *ACS Appl. Mater. Interfaces*, 2021, **13**, 47163–47173.
26 J. Zhou, *et al.*, *Energy Storage Mater.*, 2019, **22**, 256–264.
27 N. Soontornnon, K. Kimura and Y. Tominaga, *ACS Appl. Energy Mater.*, 2024, **7**, 4190–4199.
28 M. Sasikumar, *et al.*, *J. Alloys Compd.*, 2021, **882**, 160709.
29 *BIOVIA Materials Studio 7.0*, Dassault Systèmes, San Diego, 2014.
30 H. Sun, *J. Phys. Chem. B*, 1998, **102**, 7338–7364.
31 H. Sun, *et al.*, *J. Mol. Model.*, 2016, **22**, 47.
32 O. Amrhar, *et al.*, *J. Mol. Liq.*, 2023, **377**, 121554.
33 Q. Ibrahim and R. Akbarzadeh, *J. Mol. Model.*, 2020, **26**, 165.
34 M. H. Samat, *et al.*, *Results Phys.*, 2016, **6**, 891–896.
35 H. Qiu, *et al.*, *Angew. Chem.*, 2022, **134**, e202113086.
36 N. J. J. de Klerk and M. Wagemaker, *ACS Appl. Energy Mater.*, 2018, **1**, 5609–5618.